remote sensing

Article

Global Trends in Exposure to Light Pollution in Natural Terrestrial Ecosystems

Jonathan Bennie *,†, James P. Duffy †, Thomas W. Davies, Maria Eugenia Correa-Cano and Kevin J. Gaston

Environment and Sustainability Institute, University of Exeter, Cornwall Campus, Penryn, Cornwall TR10 9FE, UK; E-Mails: james.philip.duffy@gmail.com (J.P.D.); thomas.davies@ex.ac.uk (T.W.D.); mec211@exeter.ac.uk (M.E.C.-C.); k.j.gaston@exeter.ac.uk (K.J.G.)

† These authors contributed equally to this work.

* Author to whom correspondence should be addressed; E-Mail: j.j.bennie@exeter.ac.uk; Tel.: +44-132-625-9476.

Abstract: The rapid growth in electric light usage across the globe has led to increasing presence of artificial light in natural and semi-natural ecosystems at night. This occurs both due to direct illumination and skyglow - scattered light in the atmosphere. There is increasing concern about the effects of artificial light on biological processes, biodiversity and the functioning of ecosystems. We combine intercalibrated Defense Meteorological Satellite Program's Operational Linescan System (DMSP/OLS) images of stable night-time lights for the period 1992 to 2012 with a remotely sensed landcover product (GLC2000) to assess recent changes in exposure to artificial light at night in 43 global ecosystem types. We find that Mediterranean-climate ecosystems have experienced the greatest increases in exposure, followed by temperate ecosystems. Boreal, Arctic and montane systems experienced the lowest increases. In tropical and subtropical regions, the greatest increases are in mangroves and subtropical needleleaf and mixed forests, and in arid regions increases are mainly in forest and agricultural areas. The global ecosystems experiencing the greatest increase in exposure to artificial light are already localized and fragmented, and often of particular conservation importance due to high levels of diversity, endemism and rarity. Night time remote sensing can play a key role in identifying the extent to which natural ecosystems are exposed to light pollution.

1. Introduction

The past century has witnessed rapid growth in the proportion of the globe that is subject to artificial light at night [1]. The development of electric lighting and the spread of both grid-based and locally generated electricity have made the widespread illumination of human settlements, roads, and industrial infrastructure possible. An unintended repercussion of this process has been the illumination of natural and semi-natural ecosystems, both through direct illumination of the environment surrounding light sources and scattered light in the atmosphere, or skyglow, which may extend the ecological effects of light pollution many tens to hundreds of kilometres beyond urban areas [2].

The intrusion of artificial light into ecosystems is of concern because there is evidence that this can have profound effects on wildlife, including plants, invertebrates, fish, amphibians, reptiles, birds and mammals [3–8], and may have effects on key ecological processes and ecosystem services [9]. Artificial light alters the natural daily, monthly and seasonal rhythms of light and dark under which species have evolved and obscures the view of the night sky that animals may use as cues for navigation; it can disrupt natural circadian rhythms, alter the activity patterns of diurnal and nocturnal animals, interfere with movement and migration in many species, and alter the timing of key events such as flowering, budburst and reproduction. However, while several studies have considered the regional changes in artificial light [10–12], it is not clearly known which types of natural ecosystem have the greatest exposure globally to the spread of artificial light.

In addition to providing a measurement of emitted light itself [1,10,13], satellite images of artificial light at night have been shown to be a proxy measure of urbanization, human population density and economic activity at national and regional scales [14–18]. From the perspective of biodiversity conservation, satellite-sensed nighttime lights represent a measure not only of the influence of artificial light, but also of other threats associated with biodiversity loss, such as habitat fragmentation and loss, industrial pollution, resource extraction and human-wildlife conflict.

The Defense Meteorological Program Operational Linescan System (DMSP/OLS), produced and distributed by the NOAA National Geophysical Data Center, provides the longest time series of publicly available data of remotely sensed nighttime lights. While higher resolution, calibrated data are available from the day-night band of the Visible Infrared Imaging Radiation Suite (VIIRS) onboard the Suomi National Polar-orbiting Partnership (Suomi NPP) satellite since 2012 [19], DMSP/OLS nighttime lights data remain highly valuable as a source for detecting longer term trends in the distribution of artificial light at night. Quantifying changes is complicated by the lack of calibration between sensors and constant (but unknown) adjustment of the gain control of the optical instrument to provide consistent imagery of cloud. Nevertheless, careful intercalibration of the data can help to standardize the images and minimize both error and bias in order to map and detect changes over time [15,20,21]. Here we use a robust regression technique, quantile regression on the median [10] to intercalibrate DMSP/OLS images and detect changes in brightness over the period 1992 to 2012 (full details given in Methods section). We combine these data with information on the global distribution of natural and semi-natural ecosystem types, derived from

high resolution (1 km) remotely sensed land cover data and the boundaries of terrestrial ecoregions (Figure 1). We use a threshold of 3 intercalibrated Digital Number (DN) units to define areas of detectable increasing or decreasing brightness. We then assess which global ecosystems have the most rapidly increasing exposure to artificial light pollution for the period 1992 to 2012.
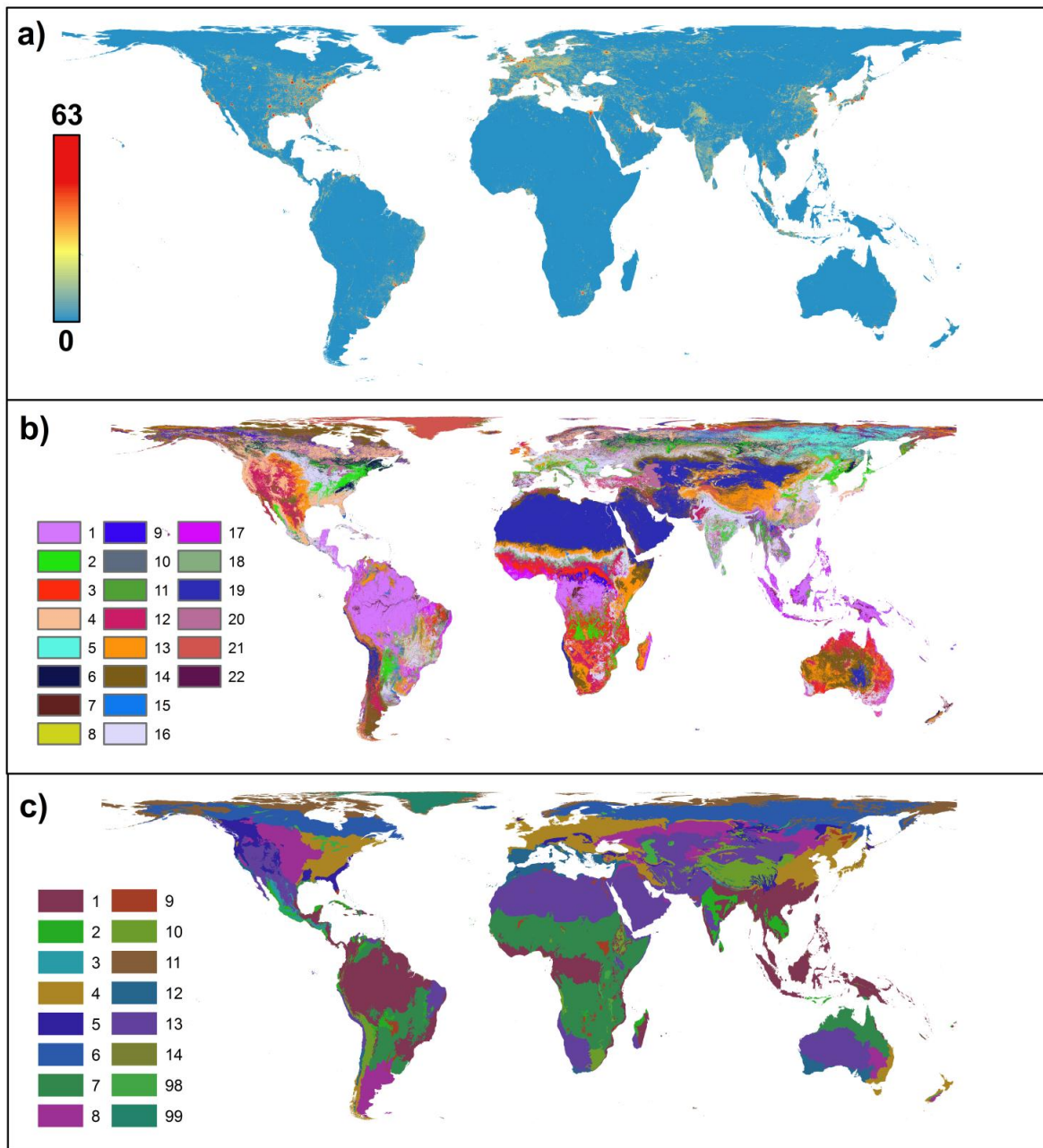

Figure 1. (**a**) Global nighttime lights image from DMSP data, 2012; (**b**) Global landcover from GLC2000, aggregated from 1 km resolution; (**c**) Global terrestrial ecoregions from World Wildlife Fund (WWF). Categories in panels b and c are coded as in Table 1.

Table 1. Classes of landcover and ecoregion used to define global ecosystem types in this study.

GLC Global Landcover Class	WWF Terrestrial Ecoregion
1. Tree Cover, broadleaved, evergreen	1. Deserts and xeric landscapes
2. Tree Cover, broadleaved, deciduous, closed	2. Tropical/subtropical moist broadleaf forests
3. Tree Cover, broadleaved, deciduous, open	3. Tropical/subtropical dry broadleaf forests
4. Tree Cover, needle-leaved, evergreen	4. Tropical/subtropical coniferous forests
5. Tree Cover, needle-leaved, deciduous	5. Temperate broadleaf and mixed forests
6. Tree Cover, mixed leaf type	6. Temperate coniferous forest
7. Tree Cover, regularly flooded, fresh water (& brackish)	7. Boreal forests/Taiga
8. Tree Cover, regularly flooded, saline water	8. Tropical/subtropical grasslands, savannas and shrublands
9. Mosaic: Tree cover/Other natural vegetation	9. Flooded grasslands and shrublands
10. Tree Cover, burnt	10. Tundra
11. Shrub Cover, closed-open, evergreen	11. Mangroves
12. Shrub Cover, closed-open, deciduous	
13. Herbaceous Cover, closed-open	
14. Sparse Herbaceous or sparse Shrub Cover	
15. Regularly flooded Shrub and/or Herbaceous Cover	
16. Cultivated and managed areas	
17. Mosaic: Cropland/Tree Cover/Other natural vegetation	
18. Mosaic: Cropland/Shrub or Grass Cover	
19. Bare Areas	
20. Water Bodies (natural & artificial)	
21. Snow and Ice (natural & artificial)	
22. Artificial surfaces	

2. Results and Discussion

All natural ecosystems considered here have experienced an increase in exposure to artificial light over this time period (Figure 2). Because areas classified in the GLC2000 dataset as "artificial surfaces" or "cultivated and managed areas" were excluded from this analysis, only a very small proportion of any ecosystem type was exposed to light at the saturation level of the sensors (the highest proportion was 0.03% at 60 DN or above, with saturation at 63 DN). We define a change in exposure of each global ecosystem type as the proportion of its area that has experienced an increase or decrease in brightness of more than 3 units (following [10]). The most marked increases are within Mediterranean ecosystems—these areas include both the Mediterranean basin itself and four other areas with a Mediterranean-type climate, typified by summer drought and a relatively mild, wet winter period, including the Cape region of South Africa, Southwest Australia, Chilean Matorral and Californian chaparral and woodlands. Mediterranean-type ecosystems harbour many "hotspots" of biodiversity and endemism, particularly for plant species—it is estimated that the Mediterranean ecoregion covers just 2% of the world's surface area but contains 20% of the world's plant species [22]. The Cape floristic region alone contains an estimated 9000 plant species, 69% of which are endemic to the region [23–25]; the South-West botanical province of Western Australia contains around 5700 plant species, 79% of which are endemic [25]. Twenty one percent of grassland and shrubland, 21% of broadleaf forest, 30% of broadleaf and needleleaf forest and 40% of mixed

forest within the Mediterranean biome have experienced detectable increases in nighttime lights. When areas which contain a mosaic of mixed natural ecosystems and agricultural land are included, 45% have experienced a detectable increase. Figure 3a,b illustrate increases in the extent of exposure to artificial light.

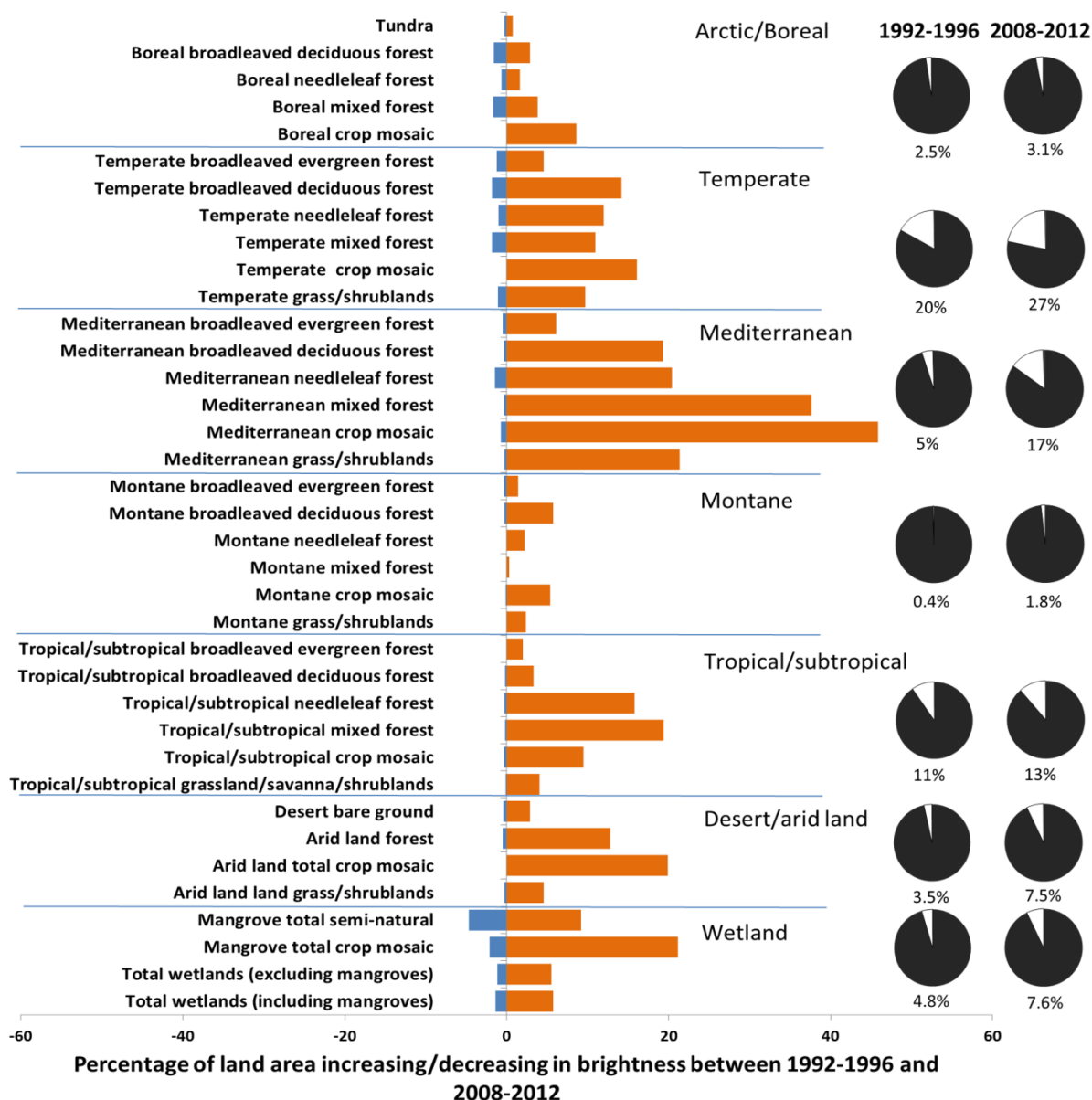**Figure 2.** Horizontal bars show the percentage of total land surface area occupied by each ecosystem type for which artificial light was detected to increase (orange) and decrease (blue) by more than 3 Digital Number (DN) units between the time periods 1992–1996 and 2008–2012. Pie charts show the proportion of the natural ecosystems within each biome that had a brightness of 6 DN or greater.
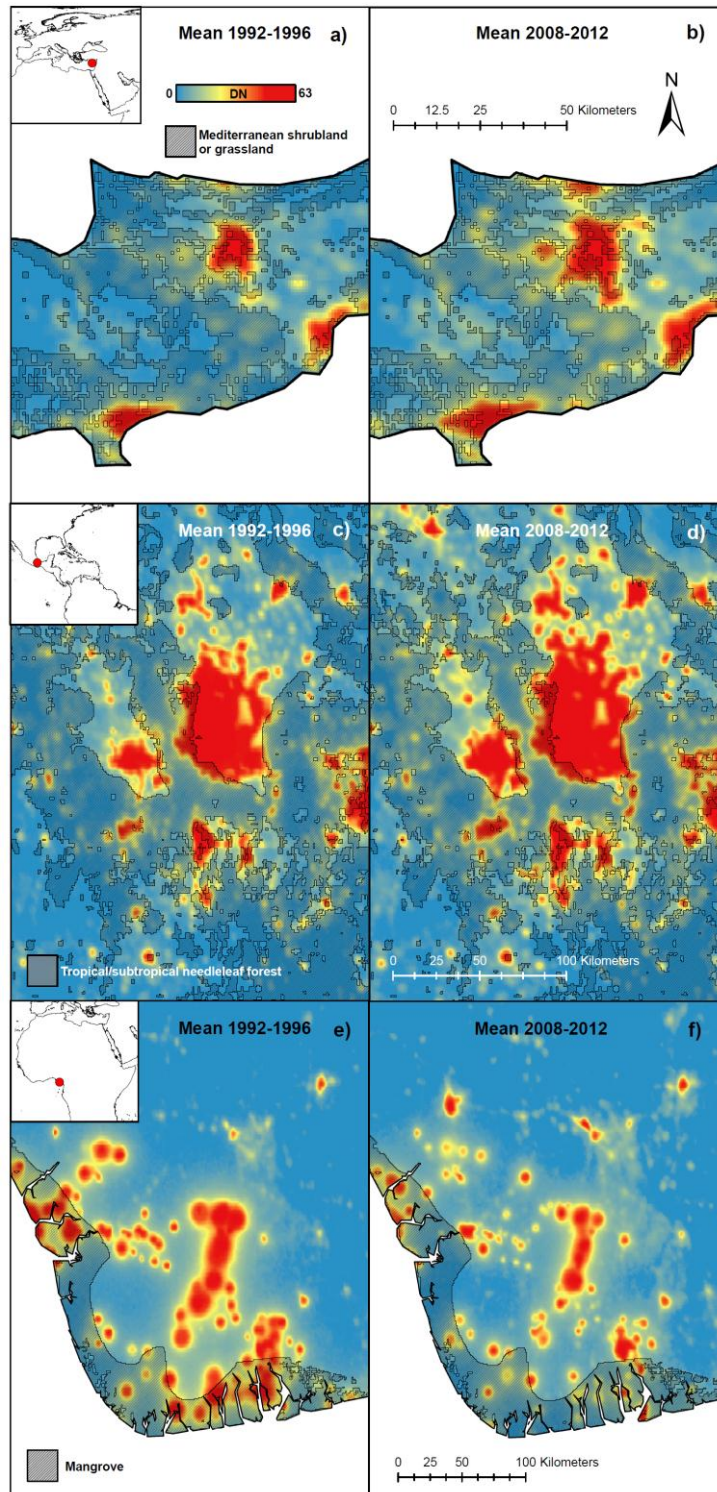
Figure 3. Selected regions illustrating encroachment of light onto natural and semi-natural ecosystems. (**a**,**b**) central Cyprus, with colour shading representing light intensity from intercalibrated DMSP/OLS data from (**a**) 1992–1997 and (**b**) 2008–2014. Cross hatched area shows the distribution of Mediterranean grassland or shrubland; (**c**,**d**) central Mexico, including Mexico City, for the same time periods. Cross hatched area shows the distribution of subtropical needleleaf and mixed forest; (**e**,**f**) the Niger Delta, Nigeria, showing the changing patterns of light emission due to changes in activity in the oil industry. Cross-hatched area shows the extent of coastal mangroves.

Temperate ecosystems have also experienced considerable increases in exposure to artificial light, ranging between 5% and 16% of the area for global ecosystem types. These regions largely coincide with rapid growth of artificial light in Europe, North America and China [1,10,15]. In the Tropical biome, the ecosystems that have experienced greatest increases in artificial light are the subtropical needleleaf and mixed broadleaf/needleleaf forests (16% and 19% respectively). Subtropical needleleaf and mixed forests are much more restricted in extent than broadleaf tropical and subtropical forests, being predominantly found in Central America, and often locally restricted to elevation bands between lowland broadleaf and high altitude cloud forest. They are characterized by high rates of biodiversity for the region; Mexican subtropical coniferous and mixed forests contain around 5300 species of flowering plants and nearly 1500 vertebrate species and contain 40% of the globally known species of trees of the genus *Pinus*, including 16 endemic species [26]. These ecosystems have experienced considerable loss in recent years; in Mexico of the 44 million hectares once occupied by the habitat, less than half (22 million ha) remains as primary forest, with a further 11 million ha as secondary regrowth [27]. In much of this region population growth and increasing urbanization have led to marked increases in light in the vicinity of these ecosystems (Figure 3c,d).

Within montane and boreal biomes, a comparatively low proportion of the land area (typically limited to less than 5% of each ecosystem type) has experienced a detectable increase in exposure to artificial light, as is also the case with deserts and arid grassland and shrubland, reflecting the low human population densities in these regions. In each case, higher rates of increase in brightness occur where semi-natural vegetation exists in a mosaic with agricultural land, and in arid biomes where patches of forest exist, often along watercourses where water is available for both vegetation growth and human settlements.

Wetlands have also experienced an increase in exposure to artificial lighting; this has been particularly marked in mangroves, which have experienced a 35% decline in global coverage since the 1970's [28]. Mangroves provide crucial ecosystem services to both the local and global community, including acting as nursery areas for commercially important fish species, providing coastal protection, detoxification of local water bodies, nutrient cycling, providing fuel and timber for local communities, supporting local biodiversity, and providing a significant source of carbon sequestration [29,30]. Nine percent of the global area of natural or semi-natural mangroves and 21% of areas of mixed mangrove and agriculture have seen an increase in exposure to artificial light. In wetlands and forested areas across all biomes there have been limited localized decreases in light intensity over the period, although these are small compared to the increases in brightness. This is often because human populations in these areas are typically smaller than those where natural vegetation exists in a mosaic with agricultural land, or where forest or wetland has been cleared or drained and converted to grassland, shrubland or aquaculture. For this reason fewer light sources are attributed to permanent settlements and roads, and more to temporary settlements and extractive industries such as forestry, fishing or mining. Figure 3e,f illustrates an example of this, showing the shifting nature of artificial light in the oilfields of the Niger Delta of Nigeria, where coastal mangroves have experienced both localised increases and decreases in artificial light over the study period.

3. Methods

3.1. Night-Time Lights Data

Twenty-one yearly (1992–2012) nighttime stable lights composite images were downloaded from NOAA [31]. These composites have been created with data from the Defense Meteorological Satellite Program's Operational Linescan System (DMSP/OLS). The images are nominally at 1 km resolution, but are resampled from data at equal angle of approximately 2.7 km resolution at the equator, and each pixel is represented by a digital number (DN) between zero and 63. A value of zero represents areas below the detection threshold, while the minimum recorded value is 3 and very brightly lit urban areas typically saturate at values of 63. For the years where two datasets were available, that from the most recently launched of the satellites was chosen. No onboard calibration of the sensors exists, and the time series includes data from several satellites with different sensors, so the brightness of images must be cross-calibrated carefully in order to assess any change in brightness. We used a robust regression technique, quantile regression through the median, that has previously been used for cross-calibration of DMSP/OLS images across Europe [10]. This method of cross-calibration is inherently insensitive to outlying values, and therefore less sensitive to changes in brightness within a calibration area, so long as the majority of pixels maintain similar light levels over time. Following [10] we first corrected for geolocation errors in the dataset by consecutively shifting each image by between −5 and 5 pixels in both the x (longitude) and y (latitude) directions and calculating the Pearson correlation coefficient of all pixels with the corresponding pixels of the image from a reference year, 2002, for which visual comparison with the land cover data suggested was accurately geolocated, matching coastlines and urban areas. The x and y offset combinations with the maximum correlation of all 121 comparisons were recorded and the coordinates of each image adjusted accordingly to maximise the match of spatial pattern between images.

Following correction for x- and y-shift, we intercalibrated images using 6th order polynomial quantile regression on the median, using the package "quantreg" [32] in the statistical software R [33]. The year 1994 was chosen as a base reference to which all other images were cross-referenced, as the image had the highest proportion of pixels with DNs of both zero and 63, by intercalibrating to this year all other images were rescaled to this range of detected values and no subsequent year's image was extended beyond the range between the minimum detectable signal and saturation. A calibration region was selected that included England and Wales, bounded by longtitude 5 °W and 2 °E, and latitude 50 °N, 55 °N. This region was selected because planning regulations in the UK have limited new urban developments over this period to a small proportion of the land area. The UK had a developed infrastructure of street lighting by the early 1990s—Unlike many other regions of Europe, there has been no widespread programme introducing new lighting infrastructure to existing settlements, even in remote and rural areas. Similarly, there have been relatively few major developments in the road network, either in terms of the widespread construction of new roads, or the widespread introduction of lighting to existing roads. Changes in lighting type over this period have also been localised. For these reasons, although the region as a whole has likely seen an increase in brightness, we consider that this increase has likely been concentrated within a minority of pixels, and hence robust regression techniques will be relatively insensitive to this increase. It is, however, impossible to test this assumption with data available for the time period of this study—although in future years VIIRS data [19] could be utilised to assess the stability and spatial

pattern of similar areas over time. An assessment of the robustness of the calibration method to increases in light intensity is given below in Section 3.4. Each consecutive year t from 1992 to 2012 was intercalibrated against this base year, by fitting the regression:

$$DN_{base} \sim c_{0,t} + c_{1,t}DN_t + c_{2,t}DN_t^2 \ldots . c_{6,t}DN_t^6 \qquad (1)$$

where DN_{base} is the digital number of the pixel in the base year (1994), DN_t is the digital number of the pixel in year *t*, and $c_{0,t}, c_{1,t} \ldots c_{6,t}$ are a set of six fitted regression constants used in converting raw digital numbers to a number intercalibrated against the base year.

3.2. Land Cover Data

The World Wildlife Fund's terrestrial "Ecoregions of the World" shapefile [34] was used to define broad biome types. The data are a biogeographic regionalization of Earth's terrestrial biodiversity and contains 867 ecoregions split into 14 different biomes [35].

The Global Land Cover (GLC) 2000 [36] product was used to determine land cover within the broad biome types. This project harmonises various regional windows standardised with 22 landcover types. It has been produced at a 1 km resolution and is derived from the VEGA 2000 dataset: a dataset of 14 months of pre-processed daily global data acquired by the VEGETATION instrument on board the SPOT 4 satellite.

The biome and land cover types were combined to define 43 ecosystem types (Table 2).

3.3. Processing

All data were re-projected to the Behrmann equal-area projection, and the WWF ecoregion data were split eight broad biome categories: (a) Boreal/Tundra; (b) Desert/Shrubland; (c) Flooded; (d) Mangroves; (e) Mediterranean; (f) Montane; (g) Temperate; (h) Tropical/subtropical, using ArcMap 10 (ESRI, 2011). The following was performed using the statistical package R [33] with the packages "rgdal" [37] and "raster" [38]. An average calibrated image for both the first (1992–1996) and last (2008–2012) five years was created. Then, each of the 22 landcover classes from the GLC data was in turn subset (*i.e.*, one raster created for each class) and used as a mask on both of the average light images, resulting in two images of nighttime lights per landcover class. The nine previously mentioned biome groups were then used as masks to split further the 22 images for both the start and the end of the time series. This resulted in 396 images in total.

The biome data and landcover type were combined according to Table 1, to provide high-resolution information about ecosystem type. Pixels were classified according to the most likely ecosystem. For example, pixels within the Boreal or Arctic biome that have predominantly herbaceous or shrub vegetation were interpreted as representing tundra. Pixels for which the landcover was classified as artificial surfaces, water bodies or snow and ice were not considered in this analysis, however, where pixels were classified as mosaics of cropland and natural or semi-natural vegetation, these were analysed separately. Due to the masking of artificial surfaces, urban areas were not considered in the analysis. We did not allow for changes in ecosystem type over the period.

Table 2. Classification of ecosystem type from World Wildlife Fund (WWF) biome and Global Land Cover 2000 (GLC2000) land cover type. Columns represent WWF biomes and rows represent GLC2000 land cover within the biome; text within the table represents ecosystem type used in this study. Abbreviations: Med. = Mediterranean, Mon. = Montane, Temp. = Temperate, T/S = Tropical/subtropical. NA = not classified.

	Land Cover	**Biome (WWF)**							
GLC Code	**Land Cover Classification (GLC2000)**	**Boreal/Arctic (7,12)**	**Mangrove (14)**	**Mediterranean (13)**	**Montane (11)**	**Temperate (5,6,9)**	**Tropical/subtropical (2,3,4,8)**	**Desert (1)**	**Flooded (10)**
1	**Tree cover broadleaved evergreen**	NA	Mangrove	Med. broadleaf evergreen forest	Mon. broadleaf evergreen forest	Temp. broadleaf evergreen forest	T/S broadleaf evergreen forest	Arid forest	Other wetland
2	**Tree cover broadleaved deciduous closed**	Boreal broadleaf forest	Mangrove	Med. broadleaf deciduous forest	Mon. broadleaf deciduous forest	Temp. broadleaf deciduous forest	T/S broadleaf deciduous forest	Arid forest	Other wetland
3	**Tree cover broadleaved deciduous open**	Boreal broadleaf forest	Mangrove	Med. broadleaf deciduous forest	Mon. broadleaf deciduous forest	Temp. broadleaf deciduous forest	T/S broadleaf deciduous forest	Arid forest	Other wetland
4	**Tree cover needle-leaf evergreen**	Boreal needleleaf forest	NA	Med. needleleaf forest	Mon. needleleaf forest	Temp. needleleaf forest	T/S needleleaf forest	Arid forest	Other wetland
5	**Tree cover needle-leaved deciduous**	Boreal needleleaf forest	NA	Med. needleleaf forest	Mon. needleleaf forest	Temp. needleleaf forest	T/S needleleaf forest	Arid forest	Other wetland
6	**Tree cover mixed leaf type**	Boreal mixed forest	Mangrove	Med. mixed forest	Mon. mixed forest	Temp. mixed forest	T/S mixed forest	Arid forest	Other wetland
7	**Tree cover regularly flooded, fresh water**	Boreal/Arctic wetland	Mangrove	Med. wetland	Mon. wetland	Temp. wetland	T/S wetland	Aridland wetland	Other wetland
8	**Tree cover regularly flooded, saline water**	Boreal/Arctic wetland	Mangrove	Med. wetland	Mon. wetland	Temp. wetland	T/S wetland	Aridland wetland	Other wetland
9	**Mosaic: tree cover/other natural vegetation**	Tundra	NA	Med. shrub/grassland	Mon. shrub/grassland	Temp. shrub/grassland	T/S shrub/grassland/savanna	Arid shrub/grassland	Other wetland
10	**Tree cover, burnt**	NA	NA	NA	NA	NA	NA	NA	Other wetland
11	**Shrub cover, closed-open, evergreen**	Tundra	Mangrove	Med. shrub/grassland	Mon. shrub/grassland	Temp. shrub/grassland	T/S shrub/grassland/savanna	Arid shrub/grassland	Other wetland

Table 2. *Cont.*

GLC Code	Land Cover Classification (GLC2000)	Biome (WWF)							
		Boreal/Arctic (7,12)	Mangrove (14)	Mediterranean (13)	Montane (11)	Temperate (5,6,9)	Tropical/subtropical (2,3,4,8)	Desert (1)	Flooded (10)
12	**Shrub cover, closed-open, deciduous**	Tundra	Mangrove	Med. shrub/grassland	Mon. shrub/grassland	Temp. shrub/grassland	T/S shrub/grassland/savanna	Arid shrub/grassland	Other wetland
13	**Herbaceous cover, closed-open**	Tundra	NA	Med. shrub/grassland	Mon. shrub/grassland	Temp. shrub/grassland	T/S shrub/grassland/savanna	Arid shrub/grassland	Other wetland
14	**Sparse herbaceous or sparse shrub cover**	Tundra	NA	Med. shrub/grassland	Mon. shrub/grassland	Temp. shrub/grassland	T/S shrub/grassland/savanna	Desert/semidesert	Other wetland
15	**Regularly flooded shrub and/or herbaceous cover**	Boreal/Arctic wetland	Mangrove	Mediterranean wetland	Montane wetland	Temp. wetland	T/S shrub/grassland/savanna	Aridland wetland	Other wetland
16	**cultivated and managed areas**	NA	NA	NA	NA	NA	NA	NA	NA
17	**Mosaic: cropland/treecover/other natural vegetation**	Boreal crop mosaic	Mangrove crop mosaic	Med. crop mosaic	Mod. crop mosaic	Temp. crop mosaic	T/S crop mosaic	Arid crop mosaic	Other wetland
18	**Mosaic: cropland/shrub or grass cover**	Boreal crop mosaic	Mangrove crop mosaic	Med. crop mosaic	Med. crop mosaic	Temp. crop mosaic	T/S crop mosaic	Arid crop mosaic	Other wetland
19	**Bare areas**	NA	NA	NA	Montane desert/semidesert	NA	NA	Desert/semidesert	Other wetland
20	**Water bodies**	NA	NA	NA	NA	NA	NA	NA	NA
21	**Snow and ice**	NA	NA	NA	NA	NA	NA	NA	NA
22	**Artificial surfaces**	NA	NA	NA	NA	NA	NA	NA	NA

3.4. Assessment of Error and Bias

In order to assess the level of error and bias expected within 5-year averaged cross-calibrated DMSP images, we compared cross-calibrated images derived from different satellites but for the same year, for the time period 1997 to 2001, which was not used during this study. During this period data independently derived from at least two satellites were available—DMSP-F12 and DMSP-F14 (1997 to 1999) and DMSP-F14 and DMSP-F15 (2000 to 2006). Root Mean Squared Error (RMSE), a measure of the "noise" in the dataset, and Mean Error (ME), a measure of systematic bias, were obtained for 5-year averages from 1997 to 2001 obtained from using independent sets of both the cross-calibrated data and raw, uncalibrated data. A sample of 1 million pixels was obtained from each image to calculate error statistics; pixels which had no detectable light in any image (DN = 0) were omitted to prevent the consistent detection of continuous darkness (for example in oceans) from influencing the error statistics. The uncalibrated data had a ME of 1.25 DN, while in the calibrated data this was reduced to 0.35 DN. The RMSE of both uncalibrated and calibrated data sets was similar (4.68 and 4.61 respectively). If only the areas covered by the (semi-)natural ecosystems used in this study were included (*i.e.*, omitting urban and cultivated regions in addition to consistently dark pixels), the ME was 0.32, and the RMSE was further reduced to 2.04. Using this dataset, 95.5% of all pixels were within 3 DN and 97.9% were within 4 DN following intercalibration.

To assess the effect of increases in light in the calibration region over time on the intercalibrated values, we performed two calibrations on the data for 1994 from the DMSP-F10 satellite (using the values for the same year from the DMSP-F12 satellite as a reference). In the first calibration, the calibration coefficients were calculated in the normal way. In the second, prior to calibration 50% of pixels in the DMSP-F10 image were selected and their value was increased by 50% (truncated to a maximum value of 63). The aim was to simulate a situation where a high proportion of the calibration area underwent a considerable increase in brightness. Both sets of calibration coefficients were then applied to the original DMSP-F10 image separately. A sample of 1 million pixels from was obtained from each image to calculate error statistics, omitting continuously dark, urban and cultivated pixels as above. The ME between these images was −0.66, indicating that under these conditions the images would slightly underestimate the brightness of pixels at later dates; the RMSE was 1.55. A total of 92.3% of the pixels had values within 3 DN and 97.6% within 4 DN. We consider that the quantile regression is robust to large directional changes in brightness over a high proportion of the area of the calibration region. Bias due to excessive increases in brightness within the calibration region would lead to dimmer global estimates in later years, so any observed increases in brightness are likely to be a conservative estimate of the true values.

3.5. Change Detection

Only those pixels increasing or decreasing more than a threshold of three intercalibrated DN units were considered as a change in exposure to artificial light. This threshold was found in a previous study to minimise the number of pixel clusters in which change was detected that could not be attributed to known changes in light intensity on the ground [10]. Given the low level of bias within the cross-calibrated datasets, it is unlikely that a consistent directional trend within an ecosystem type would be detected by chance using this threshold. To test the sensitivity of our results to the choice of threshold, particularly

for dark pixels which could change from 0 to 3 DN under a relatively small increase in brightness, we repeated the analysis using a higher threshold of 4 DN, and compared the proportion of the area under each ecosystem type that increased or decreased above each threshold. Using a threshold of 4 DN decreased the area of detected change (by an average of 18% for increases in brightness and 24% for decreases), but the proportion of each ecosystem type that changed was highly correlated ($R^2 = 0.991$ for increases, $R^2 = 0.973$ for decreases). We conclude that the qualitative results of this study are insensitive to a choice of a higher detection threshold for changes in brightness.

4. Conclusions

We show that all global terrestrial ecosystem types experience some degree of exposure to artificial light, and that this exposure is increasing. Those global ecosystems experiencing the most widespread increases in artificial light are already localized and fragmented [39], and may be of particular conservation importance due to high diversity, high levels of endemism and rarity. They are often at risk from a range of other pressures associated with urban encroachment, habitat loss and fragmentation, resource extraction and disturbance [28,40]. Mediterranean and temperate ecosystems, subtropical needleaf and mixed forest, and mangroves are particularly exposed to increasing levels of artificial light, as are forests in arid zones and natural vegetation wherever it occurs in close proximity to agricultural land. More natural ecosystems are likely to experience temporally dynamic patterns of light, perhaps associated with extractive industries rather than permanent settlements.

While DMSP/OLS provides the longest time series of global nighttime lights satellite data, and are currently unique in their ability to track changes in light pollution over time, VIIRS provides opportunities for monitoring light pollution at a higher spatial resolution; other sources of remotely sensed data such as photographs from the International Space Station [41] may also prove useful. However, remotely sensed upwelling light is only a proxy for biologically significant light at ground level, and trends must be treated with caution for several reasons. Firstly, the spectral response of the OLS instrument differs from that of human or animal vision, or the action spectra of biological processes. Secondly, remotely sensed upwelling light may not be strongly correlated with direct illumination of the environment and the horizontal emissions that cause the most skyglow. Finally, the spatial resolution and accuracy of DMSP/OLS imagery causes urban lights to be detected as somewhat blurred shapes—it is not clear to what extent the area over which light is detected corresponds to the area at which biologically significant light is detectable at ground level. Indeed, there is a need for both models to approximate the intensity of light detected by organisms at the surface from satellite images [1] and for an improved understanding of the intensity thresholds for biological impacts [6]. Any assessment of exposure to artificial light should ideally be complemented by an assessment of the sensitivity and resilience of different ecosystems to light pollution. Some groups of species, such as nocturnal invertebrates and bats [42–44], are known to be particularly sensitive to artificial light at night. However, the effects on populations of animals and plants, and effects at the level of the ecosystem, are poorly understood [8]. As our understanding of the ecological effects of light pollution grows, we need to combine this knowledge with careful monitoring of the extent to which light pollution is encroaching into our natural environment.

Acknowledgments

Author Contributions

Jonathan Bennie, James P. Duffy and Kevin J. Gaston conceived the study. Jonathan Bennie and James P. Duffy carried out the analysis. Jonathan Bennie wrote the first manuscript draft and all authors contributed to revisions.

Conflicts of Interest

The authors declare no conflict of interest.

References

1. Cinzano, P.; Falchi, F.; Elvidge, C.D. The first World Atlas of the artificial sky brightness. *Mon. Not. R. Astron. Soc.* **2001**, *328*, 689–707.
2. Kyba, C.C.M.; Hölker, F. Do artificially illuminated skies affect biodiversity in nocturnal landscapes? *Landsc. Ecol.* **2013**, *28*, 1637–1640.
3. Longcore, T.; Rich, C. Ecological light pollution. *Front. Ecol. Environ.* **2004**, *2*, 191–198.
4. Rich, C.; Longcore, T. *Ecological Consequences of Artificial Night Lighting*; Rich, C., Longcore, T., Eds.; Island Press: Washington, DC, USA, 2006.
5. Davies, T.W.; Duffy, J.P.; Bennie, J.; Gaston, K.J. The nature, extent and ecological significance of marine light pollution. *Front. Ecol. Environ.* **2014**, *12*, 347–355.
6. Hölker, F.; Wolter, C.; Perkin, E.K.; Tockner, K. Light pollution as a biodiversity threat. *Trends Ecol. Evol.* **2010**, *25*, 681–682.
7. Gaston, K.J.; Bennie, J.; Davies, T.W.; Hopkins, J. The ecological effects of nighttime light pollution: A mechanistic appraisal. *Biol. Rev.* **2013**, *88*, 912–927
8. Gaston, K.J.; Bennie, J. Demographic effects of artificial nighttime lighting on animal populations. *Environ. Rev.* **2014**, *22*, 1–8.
9. Lewansik, D.; Voigt, C.C. Artificial light puts ecosystem services of frugivorous bats at risk. *J. Appl. Ecol.* **2014**, *52*, 388–394.
10. Bennie, J.; Davies, T.W.; Duffy, J.P.; Inger, R.; Gaston, K.J. Contrasting trends in light pollution across Europe based on satellite observed night time lights. *Sci. Rep.* **2014**, *4*, 1–6.
11. Elvidge, C.D.; Hsu, F.-C.; Baugh, K.; Ghosh, T. National trends in satellite observed lighting: 1992–2012. In *Global Urban Monitoring and Assessment through Earth Observation*; Weng, Q., Ed.; CRC Press: Boca Raton, FL, USA, 2014; pp. 97–120.
12. Zhao, N.; Zhou, Y.; Samson, E.L. Correcting incompatible DN values and geometric errors in nighttime lights time-series images. *IEEE Trans. Geosci. Remote Sens.* **2014**, *53*, 2039–2049.

13. Butt, M.J. Estimation of light pollution using satellite remote sensing and geographic information system techniques. *GISci. Remote Sens.* **2012**, *49*, 609–621.

14. Sutton, P.C. A scale adjusted measure of "urban sprawl" using nighttime satellite imagery. *Remote Sens. Environ.* **2003**, *86*, 353–369.

15. Li, X.; Chen, X.; Zhao, Y.; Xu, J.; Chen, F.; Li, H. Automatic calibration of night-time light imagery using robust regression. *Remote Sens. Lett.* **2013**, *4*, 46–55.

16. Amaral, S.; Monteiro, A.M.V.; Camara, G.; Quintanilha, J.A. DMSP/OLS night-time light imagery for urban population estimates in the Brazilian Amazon. *Int. J. Remote Sens.* **2006**, *27*, 855–870.

17. Chen, X.; Nordhaus, W.D. Using luminosity as a proxy for economic statistics. *Proc. Natl. Acad. Sci. USA* **2011**, *108*, 8589–8594.

18. Huang, Q.; Yang, X.; Gao, B.; Yang, Y.; Zhao, Y. Application of DMSP/OLS nighttime light images: A meta-analysis and a systematic literature review. *Remote Sens.* **2014**, *6*, 6844–6866.

19. Miller, S.D.; Straka, W.; Mills, S.P.; Elvidge, C.D.; Lee, T.F.; Solbrig, J.; Walther, A.; Heidinger, A.K.; Weiss, S.C. Illuminating the capabilities of the Suomi National Polar-Orbiting Partnership (NPP) Visible Infrared Imaging Radiometer Suite (VIIRS) day/night band. *Remote Sens*. **2013**, *5*, 6717–6766.

20. Elvidge, C.D.; Baugh, K.E.; Safran, J.; Tuttle, B.T.; Howard, A.T.; Hayes, A.T.; Jantzen J.; Erwin, E.H. Preliminary results from nighttime lights detection. *Int. Arch. Photogamm. Remote Sens. Spat. Inf. Sci.* **2005**, *36*, 8–18.

21. De Miguel, A.S.; Zamorano, J.; Castaño, J.G.; Pascual, S. Evolution of the energy consumed by street lighting in Spain estimated with DMSP-OLS data. *J. Quant. Spectrosc. Radiat. Transf.* **2014**, *139*, 109–117.

22. Médail, F.; Quézel, P. Hot-spots analysis for conservation of plant biodiversity in the Mediterranean basin. *Ann. Mo. Bot. Gard.* **1997**, *84*, 112–127.

23. Rouget, M.; Richardson, D.M.; Cowling, R.M.; Lloyd, J.W.; Lombard, A.T. Current patterns of habitat transformation and future threats to Biodiversity in terrestrial ecosystems of the Cape Floristic Region. *Biol. Conserv.* **2003**, *112*, 63–85.

24. Goldblatt, P.; Manning, J.C. Plant diversity of the Cape Region of South Africa. *Ann. Mo. Bot. Gard.* **2002**, *89*, 281–302.

25. Beard, J.S.; Chapman, A.R.; Gioia, P. Species richness and endemism in the western Australian flora. *J. Biogeogr.* **2000**, *27*, 1257–1268.

26. Farjon, A. *A Handbook of the World's Conifers*; Brill Academic Publishers: Boston, MA, USA, 2010.

27. Challenger, A.; Soberon, J. Los ecosistemas terrestres. In *Capital Natural de México, Volume 1: Conocimiento Actual de la Diversidad*; CONABIO: Mexico, Mexico, 2008.

28. Valiela, I.; Bowen, J.L.; York, J.K. Mangrove forests: One of the world's threatened major tropical environments. *BioScience* **2010**, *51*, 807–815.

29. Barbier, E.B.; Hacker, S.D.; Kennedy, C.; Koch, E.W.; Stier, A.C.; Silliman, B.R. The value of estuarine and coastal ecosystem services. *Ecol. Monogr.* **2011**, *81*, 169–193.

30. Donato, D.C.; Kauffman, J.B.; Murdiyarso, D.; Kurnianto, S.; Stidham, M.; Kanninen, M. Mangroves among the most carbon-rich forests in the tropics. *Nat. Geosci.* **2011**, *4*, 293–297.

31. National Oceanic and Atmospheric Administration/National Geophysical Data Center (NOAA/NGDC) Earth Observation Group. Available online: http://ngdc.noaa.gov/eog/ (accessed on 6 July 2014).

32. Koenker, R. Quantreg: Quantile Regression. Available online: http://cran.fyxm.net/web/packages/quantreg/quantreg.pdf (accessed on 30 September 2014).

33. R Core Team. *R: A Language and Environment for Statistical Computing*; R Foundation for Statistical Computing: Vienna, Austria, 2013.

34. Olson, D.M.; Dinerstein, E.; Wikramanayake, E.D.; Burgess, N.D.; Powell, G.V.N.; Underwood, E.C.; D'Amico, J.A.; Itoua, I.; Strand, H.E.; Morrison, J.C.; *et al.* Terrestrial ecoregions of the world: A new map of life on Earth. *Bioscience* **2001**, *51*, 933–938.

35. Ecoregions of the World. Available online: http://www.worldwildlife.org/publications/terrestrial-ecoregions-of-the-world (accessed on 1 August 2014).

36. Global Land Cover 2000 Database. Available online: http://bioval.jrc.ec.europa.eu/products/glc2000/products.php (accessed on 1 August 2014).

37. Bivand, R.; Keitt, T.; Rowlingson, B. Rgdal: Bindings for the Geospatial Data Abstraction Library. Available online: http://cran.univ-lyon1.fr/web/packages/rgdal/rgdal.pdf (accessed on 30 September 2014).

38. Hijmans, R.J.; van Etten, J. Raster: Geographic Data Analysis and Modeling. Available online: http://cran.stat.unipd.it/web/packages/raster/raster.pdf (accessed on 30 September 2014).

39. Wade, T.G.; Riitters, K.H.; Wickham, J.D.; Jones, K.B. Distribution and Causes of Global Forest Fragmentation. Available online: http://www.ecologyandsociety.org/vol7/iss2/art7/ (accessed on 30 September 2014).

40. Moreno-Sanchez, R.; Buxton-Torres, T.; Sinbernagel, K.; Moreno, S.F. Fragmentation of the forest in Mexico: National level assessments for 1993, 2002 and 2008. *Int. J. Statist. Geogr.* **2014**, *5*, 4–17.

41. De Miguel, A.S.; Castaño, J.G.; Zamorano, J.; Kyba, C.M.; Ángeles, M.; Cayuela, L.; Martinez, G.M.; Callupner, P. Atlas of astronaut photos of Earth at night. *Astron. Geophys.* **2014**, *55*, 4–36.

42. Rydell, J. Exploitation of insects around streetlights by bats in Sweden. *Funct. Ecol.* **1992**, *6*, 744–750.

43. Stone, E.L.; Jones, G.; Harris, S. Street lighting disturbs commuting bats. *Curr. Biol.* **2009**, *19*, 1123–1127.

44. Frank, K.D. Impact of outdoor lighting on moths: An assessment. *J. Lepid. Soc.* **1988**, *42*, 63–93.